Pis'ma v ZhETF, vol. 87, iss. 11, pp. 691 – 697

High kinetic energy jets in the Earth's magnetosheath: Implications for plasma dynamics and anomalous transport

S. Savin[1)+], E. Amata[*], L. Zelenyi[+], V. Budaev[▽], G. Consolini[*], R. Treumann[□], E. Lucek[△], J. Safrankova[°], Z. Nemecek[°], Y. Khotyaintsev[◇], M. Andre[◇], J. Buechner[•], H. Alleyne[■], P. Song[▼], J. Blecki[▲], J. L. Rauch[★], S. Romanov[+], S. Klimov[+], A. Skalsky[+]

[+] Space Research Institute, Russian Academy of Sciences, 117997 Moscow, Russia,

[*] Istituto Nazionale di Astrofisica – Istituto di Fisica dello Spazio Interplanetario, 00133 Roma, Italy

[▽] Nuclear Fusion Institute, RRC Kurchatov Institute, 123182 Moscow, Russia,

[□] Munich University, 80539 Munich, Germany

[△] The Blackett Laboratory, Imperial College London, London SW7 2AZ, UK

[°] Charles University, 116 36 Praha 1, Czech Republic

[◇] Swedish Institute of Space Physics, SE-751 21 Uppsala, Sweden

[•] Max-Planck-Institut fur Sonnensystemforschung, 37191 Katlenburg-Lindau, Germany

[■] University of Sheffield, Sheffield S10 2TN, UK

[▼] University of Massachusetts, Lowell MA 01854, USA

[▲] Space Research Center, Polish Academy of Sciences, 00716 Warsaw, Poland

[★] Laboratoire de Physique et Chimie de l'Environnement, F-45071 Orleans, France

Submitted 10 April 2008
Resubmitted 29 April 2008

High kinetic energy density jets in the magnetosheath near the Earth magnetopause were observed by Interball-1 [1]. In this paper we continue the investigation of this important physical phenomenon. New data provided by Cluster show that the magnetosheath kinetic energy density during more than one hour exhibits an average level and a series of peaks far exceeding the kinetic energy density in the undisturbed solar wind. This is a surprising finding because in equilibrium the kinetic energy of upstream solar wind should be significantly diminished downstream in the magnetosheath due to plasma braking and thermalization at the bow shock. We suggest to resolve the energy conservation problem by the fact that the non-equilibrium jets appear to be locally superimposed on the background equilibrium magnetosheath, and thus the energy balance should be settled globally on the spatial scales of the entire dayside magnetosheath. We show that both the Cluster and Interball jets are accompanied by plasma super-diffusion and suggest that they are important for energy dissipation and plasma transport. The character of the jet- related turbulence strongly differs from that of known standard cascade models. We infer that these jets may represent the phenomenon of general physical occurrence observed in other natural systems, like heliosphere, astrophysical and fusion plasmas [2 – 10].

PACS: 52.40.Hf, 52.30.−q, 52.40.−w

The region downstream of a supercritical collisionless shock, the magnetosheath (MSH), is known to be in a highly disturbed turbulent state [1 – 3]. The undisturbed solar wind (SW) streams with supermagnetosonic velocity $V > c_{\rm ms}$ at magnetosonic Mach number up to $M_{\rm ms} \sim 15$. At the Earth's bow shock (BS) the SW decelerates to Mach numbers $M_{\rm ms} < 1$, thermalizes and, when entering the MSH, is compressed by roughly a factor 4. The flow downstream of the BS is highly disturbed and turbulent. However, the MSH is not spacious enough for the turbulence to reach quasi-stationarity. It remains not fully developed, intermittent and structured in time and space. In this framework, high energy density jets are been observed in the past in the magnetosheath [1, 5]. As a development of such earlier researches, we have found more than 140 events

[1)] e-mail: ssavin@iki.rssi.ru

of anomalously high kinetic energy density in the MSH during 20 orbits of Interball-1, Cluster, Polar and Geotail. Here we concentrate on two MSH crossings, by Interball-1 and Cluster [11], respectively, characterised by bursts of extraordinary high ion flux and kinetic energy density.

Fig.1 shows an example of intermittent MSH jets [15] as observed by Interball-1 on March 29, 1996. The thin

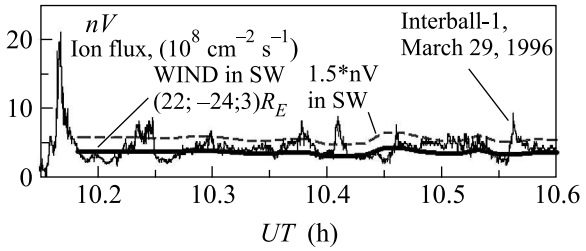

Fig.1. Ion flux (thin line) in the Turbulet Boundary Layer (TBL) near the magnetopause as measured by Interball-1 at (4.6; 2.8; 10.2) R_E GSM on March 29, 1996. The thick line shows SW ion flux measured by WIND at (22; −24; 3) R_E. The WIND flux multiplied by 1.5 is also showen by the dashed line, as a rough MHD proxy for the MSH flow

line shows the plasma flux measured by the onboard Faraday cup instrument [5] with a time resolution of 1/16 s. The plasma flow provides direct estimates for the plasma transport (cf. Fig.4). The thick line gives the SW upstream flow from WIND, while the dashed line represents a proxy for the MSH flow from MHD prediction. One can see a number of ion flux spikes much higher than the equilibrium MSH flow (dashed line). Excluding the jets, the observed flux appears to be lower than expected in the MSH by a factor ~ 1.5, as it roughly matches the SW flux. Similar matching to the SW flux has been found in the middle MSH for about 10 Interball-1 and Cluster cases. Thus, the jets look to carry the flux difference, providing the flow balance towards the MHD prediction.

Fig.2 shows kinetic energy density W_k, plasma density N, velocity V and magnetic pressure W_b from the Cluster 1 spacecraft and SW kinetic energy density W_{kSW} from WIND from 09:00 to 11:00 UT on March 27, 2002, when Cluster entered the magnetosheath inbound from the SW close to the southern magnetospheric cusp region. This MSH crossing has been analyzed previously in view of reconnection in the MSH at scales of ~ 100 km corresponding to thin current sheets [12], while here we concentrate mostly on scales larger by at least one order of magnitude. Cluster enters the MSH from the SW at about 09:35 UT. The SW as seen by the WIND spacecraft outside the foreshock at this time was very quiet with kinetic energy density practically constant

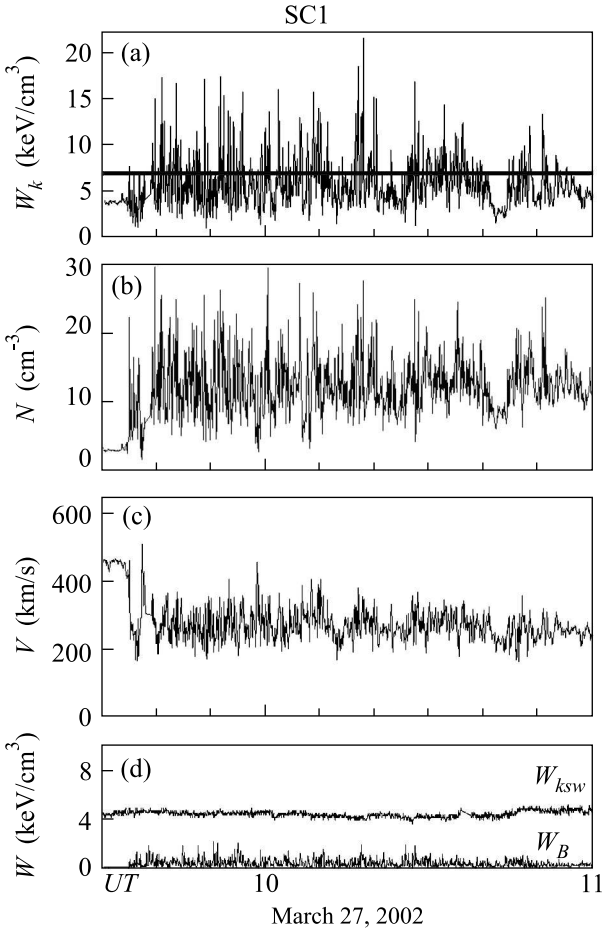

Fig.2. The Cluster 1 MSH crossing of 27 March 2002 (see in [12] the orbit; GSM $Y \sim -6R_E$). The panels (a)–(c) show 4s resolution kinetic energy density $W_k = 0.5 m_p N V^2$ (m_p being the proton mass), ion density N, and velocity V .Panel (d) shows the kinetic energy density measured by WIND in the solar wind and the Cluster 1 magnetic pressure $W_b = B^2/2\mu_0$. The horizontal thick line in panel a corresponds to the vertical dashed line defined in Fig.3

at ~ 4.5 keV/cm^3, as shown by the thick curve in the bottom panel. The SW can be considered to be uniform over the distance between WIND and the Sun-Cluster line ($\sim 8R_E$). The average SW speed, particle and kinetic energy densities were $\langle V_{\rm sw}\rangle \sim 470$ km/s, $\langle N_{\rm sw}\rangle \sim 4\,{\rm cm}^{-3}$ and $\langle W_{\rm ksw}\rangle \sim 4.5$ keV/cm^3. Compared to the SW (first 5 min at the left of Fig.2) the MSH plasma exhibits an extremely high level of fluctuations. As shown in the central panels of Fig.2, the W_k peaks result from a combination of peaks in N and in V^2 and are usually dominated by those in N, corresponding to plasma compressions moving at enhanced MSH speeds. After 11 UT the level of MSH fluctuations greatly reduced, while the upstream solar wind plasma parameters did not change significantly.

Fig.3 shows the Probability Density Functions (PDFs) of the MSH kinetic energy density for the

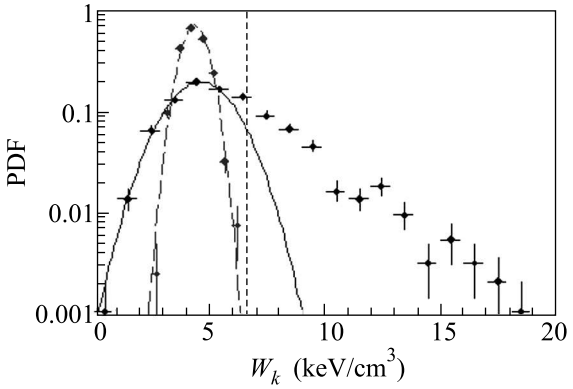

Fig.3. Semi-log plot of the Probability Density Functions (PDFs) of the MSH kinetic energy density W_k for two periods: 09:40-10:40 UT (dots with error bars) and 11:00-11:54 UT (the dots on dashed line). The dashed and solid line are Gaussian best fits of the 11:00-11:54 UT PDF and of the 09:40-10:40 UT PDF left side ($W_k < 6\,\mathrm{keV/cm^3}$), respectively. The vertical dashed line indicates the threshold chosen for the detection of jets

09:40-10:40 UT period, i.e. the central part of Fig.2 characterized by the large W_k peaks, and for 11:00-11:54 UT (the dots on the dashed line), which we use as a reference period for a quieter MSH. It is clear that the two MSH regimes are completely different, while the solar wind energy density was the same in the two cases. A Gaussian equilibrium distribution is found to fit the "quiet" 11:00-11:54 UT PDF (dashed line). Conversely, for the 09:40-10:40 UT period the PDF shows a clear non-Gaussian shape with a tail extending to very large values of the energy density. The strong asymmetry of the 09:40-10:40 UT PDF points towards the presence of an extra non-equilibrium contribution arising from the plasma jets: a Gaussian fit, similar to that of 11:00-11:54 UT PDF, can be performed only for the left-hand side ($W_k < 6\,\mathrm{keV/cm^3}$) of the 09:40-10:40 UT PDF (solid curve), whose peak, W_k^0, and variance, σ_G, are such that $W_k^0 + 1.5\sigma_G = 6.7\,\mathrm{keV/cm^3}$. This energy density is marked as a vertical dashed line, which falls above all the PDF points for the 11:00-11:54 UT period. Therefore, it looks reasonable to consider the $W_k = 6.7\,\mathrm{keV/cm^3}$ threshold as the maximum kinetic energy density which one should expect for the equilibrium MSH plasma between 09:40 and 10:40 UT and draw it as a horizontal line in panel a of Fig.2. We note that the $0 < W_k < 6.7\,\mathrm{keV/cm^3}$ interval contains more than 68% of the W_k values and that the chosen threshold is $\sim 1.5\langle W_{\mathrm{kSW}}\rangle$ (where W_{kSW} is the SW kinetic energy density).

Turning back again to Fig.2, we notice that the thick threshold line is exceeded by quite a number of peaks in W_{k} by up to a factor of 3. In the following we concentrate our analysis on such peaks, which we call 'High Kinetic energy density Plasma Jets' (HKPJ). This definition is based on much higher threshold in kinetic energy density than for the earlier published cases of enhanced MSH flows [1, 4].

Under the stable SW conditions monitored by WIND, this quantitative definition infers that all HKPJs be of MSH or BS origin. Close inspection of the peaks has led to count 83 HPKJs during the period under study, having an average duration of 28 s (i.e. ~ 6000 km). In 77 cases a velocity increase relative to the ambient MSH is also seen. In 26 cases density enhancements are seen close to the HKPJ edges suggesting piling up of the ambient MSH plasma. In 57 cases the N and V peaks do not coincide. The W_k peak corresponds in time to the $N(V)$ peak in 29 (10) cases.

We remark that a part of the SW kinetic energy transforms at the BS into the thermal one, yielding a decrease of the kinetic energy density $W_{\mathrm{kSW}} \sim 4.5\,\mathrm{keV/cm^3}$, which one can compare with $\langle W_{\mathrm{k}}\rangle \sim 6\,\mathrm{keV/cm^3}$ (with the standard variance $\sigma = 2.6$) in the disturbed MSH. We would address this paradox as following: the equilibrium MSH subpopulation with $\langle W_{\mathrm{kMSH}}\rangle \sim 4\,\mathrm{keV/cm^3}$ (see dashed line Fig.3) is superimposed by the transient jets, having $W_k > 6.7\,\mathrm{keV/cm^3}$ and respective measured $\langle W_{kJ}\rangle \sim 9\,\mathrm{keV/cm^3}$ ($\sigma \sim 2.4$). Thus, one gets approximately the measured average value $\langle W_{\mathrm{k}}\rangle$ for the mixture of equilibrium and non-equilibrium subpopulations. Really, this is not a simple mixture of non-interacting plasmas as in the disturbed region the parallel and perpendicular ion temperatures are equal and have much wider spread into the lower magnitude region, while in the quiet MSH the perpendicular temperature strongly dominates (not shown). The jets most probably are transient both in space and time (cf. Fig.1–3), thus the energy conservation should be settled only on a time interval over several characteristic time intervals for the jets and only at a spatial scales comparable with the entire dayside MSH.The latter conforms to the fact that the ion flux near the magnetopause (see Fig.1) has the background level much below the MHD proxy, contrary the ion flux at 09:40-10:40 UT (cf. Fig.2) being in average in about 1.5 time higher than its MHD proxy from the SW WIND data (not shown). I.e. the flux closer to MP (Fig.1, remember also about 10 such cases mentioned above) can be considerably smaller than the MHD proxy, while the flux just inside BS could conversely exceed the MHD proxy. For a further quantitative check of this point one needs

to find a fortunate case in Cluster and THEMIS data and run MHD model.

Considerations, similar to that of W_k, are valid also for the respective Mach numbers M_{ms}: between 11:00 and 11:20 UT $\langle M_{ms}\rangle \sim 1$ ($\sigma \sim 0.5$); between 09:42 and 11:00 UT $\langle M_{ms}\rangle \sim 1.34$ ($\sigma \sim 0.27$). The latter suggests that a super-magnetosonic population with $W_k > 6.7\,\mathrm{keV/cm^3}$ and $\langle M_{ms}\rangle \sim 1.62$ with $\sigma \sim 0.25$, adds to that with low M_{ms} giving the mentioned above average value.

Further to the analysis we made for $W_k > 6.7\,\mathrm{keV/cm^3}$ we concentrated on 33 stronger HKPJs having $W_k > 10\,\mathrm{keV/cm^3}$ (i.e. $> 1.5\sigma$ over the $\langle W_k\rangle$ in the MSH), for which we studied the distribution of angles $\alpha = a\sin(V_z/|\mathbf{V}|)$ and found that for 36% of the cases $\mathbf{V}$ was deflected from the average MSH flow towards the MP by $> 16^0$, while for 12% of the cases $\mathbf{V}$ was deflected by $> 34^0$. The strongest HKPJs have $\langle W_k\rangle \sim 16\,\mathrm{keV/cm^3}$ and a characteristic scale $\sim 6\,\mathrm{s}$, i.e. 1000–1500 km, which correspond to 3–11 proton gyroradii. Namely these strongest HKPJs represent most distinguishable new entities to which this Letter is devoted. It is most interesting to check the magnetic signatures of the HKPJs (displayed by the lower solid line in the panel d in Fig.2). The magnetic pressure W_b is very low during this passage of the MSH and is completely negligible compared with the kinetic energy density, in particular when compared with W_k in the jets. Moreover, in most of the observed jets the magnetic field increases do not coincide with the jet maxima, nor does the magnetic pressure exhibit a minimum in the jet centers (which would be required for a plane current layer). This makes it difficult to associate the jets uniquely with thin fast current sheets [13]. The important conclusion from this comparison is that reconnection cannot be the cause of HKPJs simply because there is no sufficient energy stored in the magnetic field.

The observation of such high kinetic energy density jets in the intermittent turbulence of the MSH plasma [13] poses a serious problem to understand possible mechanisms of their formation. To this regard, we note that the dynamic interaction in the MSH plasma, that is bounded at one side by the BS and at the opposite side by the MP, is non-uniform and intrinsically transient, as the plasma is still evolving from the shocked to a statistically equilibrium turbulent state. In the course of this evolution, it seems that processes may occur which concentrate the free energy in the still underdeveloped turbulence and focus the plasma into jets of very high kinetic energy density, in a way that is relatively independent of the state of the upstream SW. It is also probable that such processes are favoured by the presence of moving boundaries [4]. How this proceeds, with ion kinetic energy rise inside the jets being comparable with ion temperature drop (cf. [18]), remains unclear. To that extent, we first remind a mechanism, based on inertial-drift plasma acceleration by non-uniform electric field structures [1, 4, 19] almost standing in the MP frame, which can account for the enhanced jet velocities. Such structures constitute wave interference patterns in the MSH [19] with electric field forcing the incident flow into an equilibrium state that adjusts for the presence of the moving boundaries [4] and transfers the momentum downstream the MSH by means of jets' formation.

Now we would like to discuss in more details the implications of HKPJs for the turbulence and transport characteristics. As was mentioned above, the substantial part of the HKPJs in Fig.2 can hit the MP, and all such HKPJs with $W_k > 6.7\,\mathrm{keV/cm^3}$ pierce through the downstream MP (cf. [30]), having the total pressure (magnetic + thermal) well below $6\,\mathrm{keV/cm^3}$. And we suggest that such jets, detected in front of MP (see Fig.1 and [1]), with their specific statistical properties could provide the respective diffusion-like transport across the MP. Thus, further on we make use of statistical properties of different signals in the extended regions with HKPJs (cf. Fig.1,2), to explore the transport properties (self-similarity scalings) in this important region.

The statistical properties are studied by analyzing the structure functions (i.e. the moments of the probability distribution function, PDF, see Fig.3 and, e.g., [6]) of different orders q versus time lag τ from the experimental time series $X(t)$: $S_q(\tau) = \langle|\delta_\tau X(t)|^q\rangle$, $\delta_\tau X(t) = X(t+\tau) - X(t)$, $\langle\ldots\rangle$ stands for statistical averages, from the experimental time series X(t). Statistical self-similarity of the type $S_q(\tau) \sim \tau^{\zeta(q)}$ can be expected in the inertial range. For the isotropic fully developed 3D turbulence (described by Kolmogorov's K41 model [22]), the scaling exponents $\zeta(q) = q/3$ [3, 15]. We analyze the data, displayed in Fig.1 and 2 (at 09:40-10:40 UT on March 27, 2002), by fitting the parameters β and Δ of log-Poisson turbulent cascade model [25] for different experimental scalings:

$$\zeta(q) = (1-\Delta)\frac{q}{3} + \frac{\Delta}{1-\beta}\left[1 - (\beta)^{\frac{q}{3}}\right], \qquad (1)$$

The β and Δ parameters characterize intermittency and singular dissipative structures, respectively. For 3D isotropic turbulence Z.S. She and E. Leveque (SL) have proposed $\beta = \Delta = 2/3$ [5]. The Iroshnikov-Kraichnan model [23, 24] leads to a reduction of the problem symmetry. A Kolmogorov-type energy spectrum in magnetized plasma can also be derived in an assumption of a

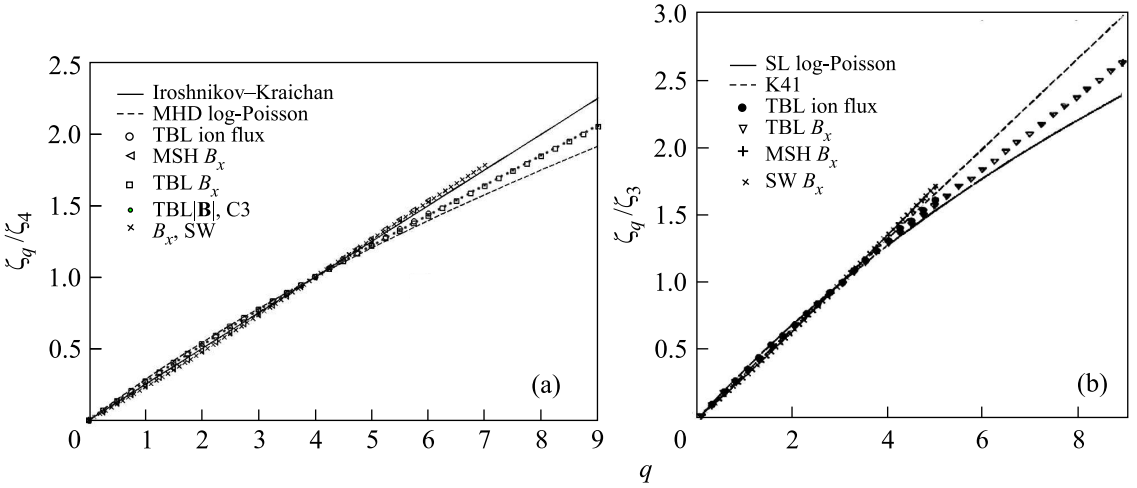

Fig.4. (a) Relative exponents $\zeta(q)/\zeta(4)$ dependence on its order q for Interball-I (TBL ion flux, MSH B_x, TBL B_x), Cluster 3 (TBL $|\mathbf{B}|$, C3) and Geotail (B_x, SW) data (see the respective symbols in the right bottom corner and text for details). Solid line is the Iroshnikov-Kraichnan scaling $q/4$ [23, 24]. Dashed line is the log-Poisson model of She-Leveque modified in MHD case to account for the IK phenomenology [27]. (b) Dependence of the scaling ratio $\zeta(q)/\zeta(3)$ on its order q versus that of Kolmogorov K41 (a dashed line) and that of the log- Poisson She-Leveque model (SL, [28]), describing the developed 3D turbulence (a solid line). The symbols in the right bottom corner mark different experimental signals for Interball-I (TBL ion flux, MSH B_x, TBL B_x) and Geotail (B_x, SW) data

critical balance [26]. The log-Poisson model was modified for MHD case to account for the IK phenomenology [27] (MHD IK). This phenomenology depends on the dimension of the most intensely dissipative structures and their scaling (the IK model supposes two-dimensional sheet-like dissipative structures [27]).

To test the IK hypothesis we display in Fig.4a the relative exponents $\zeta(q)/\zeta(4)$ dependence from the q for different spacecraft data (cf. [15]). The scaling of a GSE magnetic component B_x in MSH outside TBL on June 19, 1998 is close to the IK scaling $q/4$. The same is true for the SW B_x from Geotail recorded at the same time interval on June 19, 1998, as the B_x in TBL on Interball-1 [1, 15]. It infers that generally the BS does not change substantially the SW statistical properties. In contrast to the simultaneous SW data, the TBL B_x data from Interball-1 [1] are deviated strongly from the IK scaling. For the extremely disturbed TBL on Cluster 3 closer to the BS (cf. Fig.2) surprisingly one sees practically coinciding scaling with that of Interball-1 near the MP.

In the finite pressure plasma the magnetic fluctuations could have different properties from that of the ion flow. But scaling of the ion flow in TBL (see TBL ion flux in Fig.4a, cf. Fig.1) well fits that of the B_x. The Fig.4a demonstrates that the original IK phenomenology does not describe the scaling property of intermittent turbulence in the TBL. At the same time, they are not fitted by the MHD IK scaling [27]. Thus, the TBL turbulence is neither isotropic nor has the 2D dissipative structures.

We also look for a power-law dependence of $S_q(\tau)$ on $S_3(\tau)$, $S_q(\tau) \sim S_3(\tau)^{\zeta(q)/\zeta(3)}$, i.e. for Extended Self-Similarity (ESS, [15]). In the cases under study, [15] demonstrates the ESS properties. We compare the scaling of the S_q with the K41 and the SL models. The quiet MSH and SW scalings deviate slightly more from the K41 straight line than that of Fig.4a from the IK straight line. The TBL scalings differ from that of the K41 turbulence as much, as from the IK scaling. $\zeta(q)/\zeta(3)$ in the TBL also departs from the SL model [28]. Instead, [15] demonstrates that the TBL dissipative structures are most likely the 1D filaments.

We have checked the plasma transport properties in the jet regions by analyzing the particular cases displayed in Fig.1, 2, 4 and published in [1]. For that purpose, we display the fitted the log-Poisson parameters β and Δ in Table. [14] approximates the scaling of diffusion coefficient as $\mathcal{D}_f \propto \tau^{K(-1)}$, where $K(q) = q - \zeta(3q)$. It is a result of a considering the average over various initial walker starting positions; this is equivalent to ensemble averaging.

From Table for the scaling (1), one gets $\text{K}(-1) \approx \approx 0.33 \div 0.39$. The average displacement of a particle scales as: $\langle \delta x^2 \rangle \propto \mathcal{D}_f \tau \propto \tau^{\Psi}$, with $\Psi = 1 + \text{K}(-1) \approx \approx 1.33 \div 1.39 > 1$, that infers the super-diffusion. Note, that for the classical diffusion $\Psi = 1$, as it is the case for the MSH and SW B_x (Table, two bottom lines).

On the other hand, we also fitted the probability distribution of $\delta_\tau |\mathbf{B}|$ and $\delta_\tau V_z$ from Cluster by a Levy function $L_\alpha = (1/\pi) \int \exp(-\gamma \tau^\alpha) \cos(\tau x) dx$ at various τ.

Data type	Δ	β	$K(-1)$
TBL near MP, B_x, Interball-1	0.24	0.38	0.39
TBL near MP, ion flux, Interball-1	0.2	0.36	0.36
TBL downsream BS, $\|\mathbf{B}\|$, Cluster 3	0.23	0.41	0.33
MSH, B_x, Interball-1	≈ 0	1	≈ 0
SW, B_x, Geotail (simultaneously with TBL near MP, B_x)	≈ 0	1	≈ 0

In particular, corresponding to the proton cyclotron frequency, we choose [17] $\tau = 1.4$ s and the fits yield the parameter [16–18] $\alpha \sim 1.66$ or ~ 1.8, which give [17] $\langle \delta x \rangle^2 \propto t^{2/\alpha} = t^{1.2}$ or $t^{1.11}$ for the Cluster $\delta_\tau |\mathbf{B}|$ and $\delta_\tau V_z$, respectively. For the Interball case the Levy function fitting for magnetic vector rotation angles gives [16] $\alpha \sim 1.2$, and respectively, $\langle \delta x \rangle^2 \propto t^{1.67}$.

Finally, a further analysis was performed between 09:40 and 10:40 UT based on HIA Cluster 3 ion energy [11], $\epsilon = 0.5 m_p (\delta \mathbf{V})^2$, where $\delta \mathbf{V} = \mathbf{V} - \langle \mathbf{V} \rangle$ and $\mathbf{V}$ is the 4s HIA ion velocity (cf. Fig.2). By applying the rank ordering statistics [21] to the ϵ time series, we get [17] $\langle \delta x^2 \rangle \propto t^{1.11}$.

We would like to outline that in our scaling analysis we have excluded small scales comparable or less than that of the order of proton inertial length [13] (by respective averaging or using of the data with low sampling rate), which gives unrealistic $\langle \delta x^2 \rangle$ time scalings with the power exponent over 2 [17, 14].

In spite the scaling exponents spread, all these scalings correspond to super-diffusion [17]. So qualitatively, we conclude that MSH turbulence including HKPJs exhibits signs of the plasma super-diffusion and anomalous plasma transport. It should affect the effective deceleration of the MSH flow closer to the MP (i.e. dissipate the kinetic energy in boundary layers) via carrying downflow of the momentum 'excess' by the jets [1, 19], supporting SW plasma penetration across the high-latitude MP. Note that about 20% of the strongest jets on March 27, 2002 (see Fig.2 and discussion above) are considerably deflected towards the MP from the average direction of the MSH flow, and hence these jets with $W_k \gg W_b$ at the MP could provide the super-diffusive transport inside the high-latitude magnetosphere.

One could consider the possibility that turbulent reconnection, as proposed for the 27 March, 2001 event [12, 1], provides a way for free flow of the super-magnetosonic jets (with interior Mach number $\langle M_{ms} \rangle \sim \sim 1.6$) across the subsonic background MSH, although the ambient magnetic field energy density cannot provide a substantial amount of energy density for the jet generation. Kuznetsov et al. [29] proposed Alfvénic collapse under high ion-β conditions (which holds in Fig.2) to provide a local plasma acceleration through the expulsion of plasma by the collapsing magnetic fields. As for the Fig.2, the Alfvénic collapse is not seen in the bottom panel (thus, a local acceleration via the Alfvénic collapse can be excluded), so the secondary reconnection at the jet borders looks to be operative. Similar phenomena are known from random "hot spots" in laser plasmas [20], which initiate two-dimensional self-focusing of laser beams into filaments.

To conclude this Letter, we recall that interacting moving matters in the laboratory, in fusion plasmas like the tokamak [9, 15] boundary layer or laser plasmas [20], in the heliosphere and also in astrophysical plasmas [6, 7] frequently generate localized jets of high kinetic energy density [3 – 10] exceeding the kinetic, thermal and magnetic field energy densities of the interacting components. Such systems are quite different from each other, as regards their plasma parameters and the physical process which occur in them; nevertheless, they seem to display as a common property the collimating of kinetic energy into narrow spatial regions. The dynamic plasma interaction advanced in this paper differs from the classic one [31]. The analysis of Interball and Cluster data indicates on a more sophisticated scenario of plasma flow braking. Before the final (asymptotic) plasma thermalization downstream of the BS, a number of localized HKPJ structures is formed within the MSH, which could have numerous important dynamical implications discussed above.

The correspondence between the jets and Alfvénic/magnetosonic [13] eigenstates, which are localized in density humps, is analogous to the correspondence between discrete eigenstates of the one-dimensional nonlinear Schrödinger equation whose stationary solutions are solitons [20].

In most cases the jet-flux amplitude and jet duration resemble indeed standard flow quantization. Savin et al. [1] suggested maser-like flow quantization by self-focused jets to be due to the transition of flow from a meta-stable state with super-Alfvénic velocity to a stable state with Alfvénic or sub-Alfvénic flows. The latter state permits magnetic stress balance (i.e. a force-free equilibrium) that minimizes the total energy of the flow-obstacle interaction. As a consequence, the MSH flux aims at SW flux levels (cf. the background W_k in Fig.1).

This is also the case on June 19, 1998 [1, 19]. Thus, the jets can provide the considerable input into a quasi-static flow balance in the MSH. It is a task of future investigation to illuminate the interrelation between the above mechanisms of jet generation for the different types of jets [4 – 7, 15].

Nature seems to 'prefer' highly non-uniform equilibriums with large excesses of free (in our case, kinetic) energy. The mechanism of jet generation is still barely understood, its further studying should shed light on the inherent transient dynamics of plasma streaming [6, 7, 15] and its transport properties.

This work was partially supported by INTAS # 03-50-4872, # 06-100017-8943 and # 05-1000008-8050, RFFS # 06-02-17256, # 07-02-92210-NTNIL, # 07-02-00319, ISSI, KBN # 8T12 E 016 28. We appreciate providing of the Interball-1 ion flux data by Prof. G.N. Zastenker, and the Geotail MFI team – for high-resolution magnetic data. We thank for helpful discussions A. Volosevich, S. Zhestkov, E. Churazov, S. Moiseenko.

1. S. P. Savin, L. M. Zelenyi, E. Amata et al., JETP Lett. **79**, 452 (2004).
2. D. G. Sibeck et al., Space Sci. Rev. **88**, 207 (1999).
3. F. Sahraoui, G. Belmont, L. Rezeau et al., Phys. Rev. Lett. **96**, 075002 (2006).
4. E. Amata, S. Savin, M. Andre et al., Nonlin. Proc. Geophys **13**, 365 (2006).
5. Z. Nemecek, J. Safrankova, L. Prech, et al., Geophys., Res. Lett. **25**, 1273 (1998).
6. M. C. Begelman, R. D. Blandford, M. J. Rees, Rev. Mod. Phys. **56**, 255 (1984).
7. A. I. MacFadyen, S. E. Woosley, and A. Heger, Astrophys. J. **550**, 410 (2001).
8. D. Bartolo, C. Josserand, and D. Bonn, Phys. Rev. Lett. **96**, 124501 (2006).
9. V. P. Budaev, S. Takamura, N. Ohno, and S. Masuzaki, Nucl. Fusion **46**, S181 (2006).
10. J. Merka, J. Safrankova, Z. Nemecek et al., Adv. Space Res. **25**, 1425 (2000).
11. The Cluster mission description, Ann. Geophys. **19**, No. 10/12, (2001).
12. A. Retino, D. Sundkvist, A. Vaivads et al., Nature Physics **3**, 236 (2007).
13. D. Sundkvist, A. Retino, A. Vaivads, and S. D. Bale, Phys. Rev. Lett. **99**, 025004, (2007).
14. A. V. Chechkin, R. Gorenflo, and I. M. Sokolov, Phys. Rev. E **66**, 046129 (2002).
15. V. P. Budaev, S. Savin, L. Zelenyi et al., Plasma Phys. Contr. Fusion. **50**, DOI /10.1088/0741-3335/50/1 (2008).
16. S. Savin, J. Buechner, G. Consolini et al., Nonlin. Proc. Geophys. **9**, 443 (2002).
17. R. A. Treumann, Geophys. Res. Lett. **24**, 1727 (1997).
18. S. Savin, L. Zelenyi, E. Amata et al., A Planet. Space Sci. **53**, 133 (2005).
19. S. Savin, A. Skalsky, L. Zelenyi et al., Surveys in Geophys. **26**, 95 (2005).
20. P. A. Robinson, Rev. Mod. Phys. **69**, 508 (1997).
21. D. Sornette, Critical phenomena in natural sciences. Chaos, fractals, selforganization and disorder: concepts and tools, Springer-Verlag, Berlin Heidelberg (2000).
22. A. N. Kolmogorov, Doklady Akademii Nauk SSSR **30** (4), 299 (1941) [reprinted in Proc. R. Soc. London, Ser. A **434**, 9 (1991)].
23. P. S Iroshnikov, Astron. Zh. **40**, 742 (1963) [reprinted Sov. Astron. 7, 566 (1964)].
24. R. H. Kraichnan, Phys. Fluid,s **8**, 1385 (1965).
25. B. Debrulle, Phys. Rev. Lett. **73**, 959 (1994).
26. P. Goldreich and S. Sridhar, Astrophys. J. **438**, 763 (1995).
27. W. Muller and D. Biskamp, Phys. Rev. E **67**, 066302 (2003).
28. Z. S. She and E. Leveque, Phys. Rev. Lett. **72**, 336 (1994).
29. E. A. Kuznetsov, S. Savin, F. Amata et al., JETP Lett. **85**, 288 (2007).
30. J. Lemaire and M. Roth, Space Sci. Rev. **57**, 59 (1991).
31. R. Z. Sagdeev, *Reviews of Plasma Physics*, Vol.4. Authorized translation from the Russian by Herbert Lashinsky, University of Maryland, USA. Ed. M. A. Leontovich, Published by Consultants Bureau, New York, 1966, p. 23.